NH$_2$(Ã^{2}A$_1$) AND NH(A^{3}Π) FORMATION FROM CONTINUOUS WAVE IR LASER IRRADIATION OF NH$_3$

J. MASANET, J. DESON, C. LALO, F. LEMPEREUR and J. TARDIEU DE MALEISSYE

Laboratoire de Chimie Générale, Université Pierre et Marie Curie, 4 Place Jussieu, 75230 Paris Cédex 05 (France)

(Received December 16, 1985)

Summary

Ammonia was photoexcited at 10.6 μm by a continuous wave CO_2 laser with an output power of 100 W. NH$_2$(Ã^{2}A$_1$ → X̃^{2}B$_1$) and NH(A^{3}Π → X^{3}Σ$^-$) emissions were observed. The mechanisms of formation of the two excited radicals are discussed. The variation in NH$_2$(Ã^{2}A$_1$ → X̃^{2}B$_1$) emission *vs.* ammonia pressure exhibits a maximum for $p_{NH_3} \approx 300$ Torr; this maximum is due to the equilibrium between the collisional activation and the quenching of NH$_2$(Ã^{2}A$_1$) by ammonia. The NH$_2$(Ã^{2}A$_1$) emission is strongly affected by addition of transparent gases because the rate of thermodiffusion changes with the relative pressure. Argon strongly promotes the NH$_2$ emission while helium inhibits it completely under our experimental conditions.

---

1. Introduction

Numerous studies concerning classical photolysis of ammonia obtained in the vacuum UV [1 - 8], by synchrotron radiation [9] and by UV [10 - 12] and IR [13 - 16] laser excitation have indicated that excited photofragments are formed. The observed radicals were NH$_2$(Ã^{2}A$_1$), NH(A^{3}Π), NH(b^{1}Σ$^+$) and NH(c^{1}Π); in several cases correlations with potential curves of NH$_3$ were determined.

The present work concerns the photoexcitation of ammonia followed by decomposition, under continuous wave (CW) CO_2 laser excitation at 10.6 μm. CW irradiation at between 10 and 300 W incident laser power results in the thermodiffusion of the absorbing species [17]. This effect depletes transiently the concentration of the absorbing species inside the irradiated zone and reduces the quantum yield.

The CW laser absorption creates a high pressure heat bath which is coupled with the CW laser field leading to generation of photofragments inside the irradiation zone.

$NH_2(\tilde{A}\,^2A_1)$ radical emission is observed on pumping the ammonia ν_2 bending vibration by the P20 emission line from a CO_2 laser at 10.6 μm [13 - 15] but its mode of formation is not well understood. The purpose of this work is to clarify some aspects of the mechanism of radical formation.

2. Experimental details

The CO_2 laser beam (about 100 W) at 10.6 μm was focused with an NaCl lens ($f = 11.5$ cm) in a flow system cell. The emissions were observed and analysed at right angles to the beam by a Jobin–Yvon HRP monochromator coupled with a photocounting system which included a Hamamatsu R 585 photomultiplier sensitive between 200 and 650 nm and an Ortec 9315 amplifier. The experiment was controlled overall by a CBM microcomputer.

Ammonia (purity, 99.6%) and helium, argon and nitrogen (all 99.99% pure) were purchased from Air Liquide. All the gases were used without further purification.

3. Experimental results

When ammonia is irradiated, yellow luminescence appears at pressures between 80 and 760 Torr. This emission is strictly limited to the conic volume of irradiation (Fig. 1).

3.1. $NH_2(\tilde{A}\,^2A_1 \rightarrow \tilde{X}\,^2B_1)$ emission

A spectroscopic study of the emission (Fig. 2) was performed between 400 and 650 nm; the luminescence is assigned unambiguously to the radical emission $NH_2(\tilde{A}\,^2A_1 \rightarrow \tilde{X}\,^2B_1)$ [18].
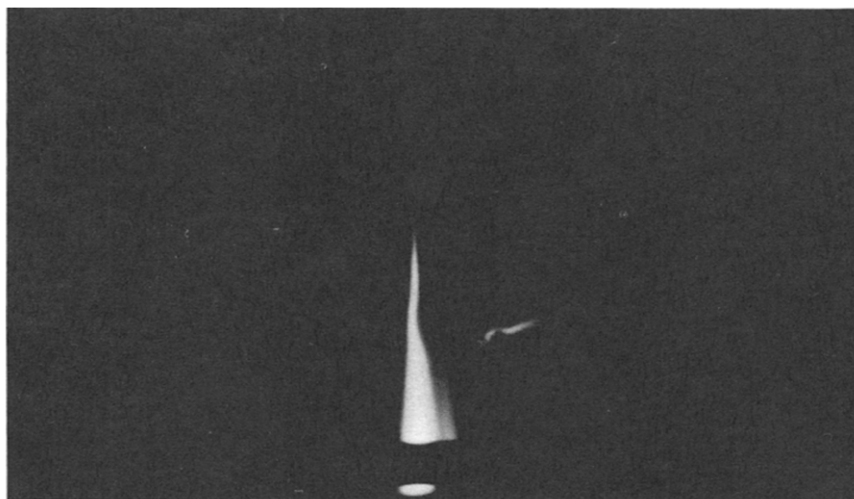

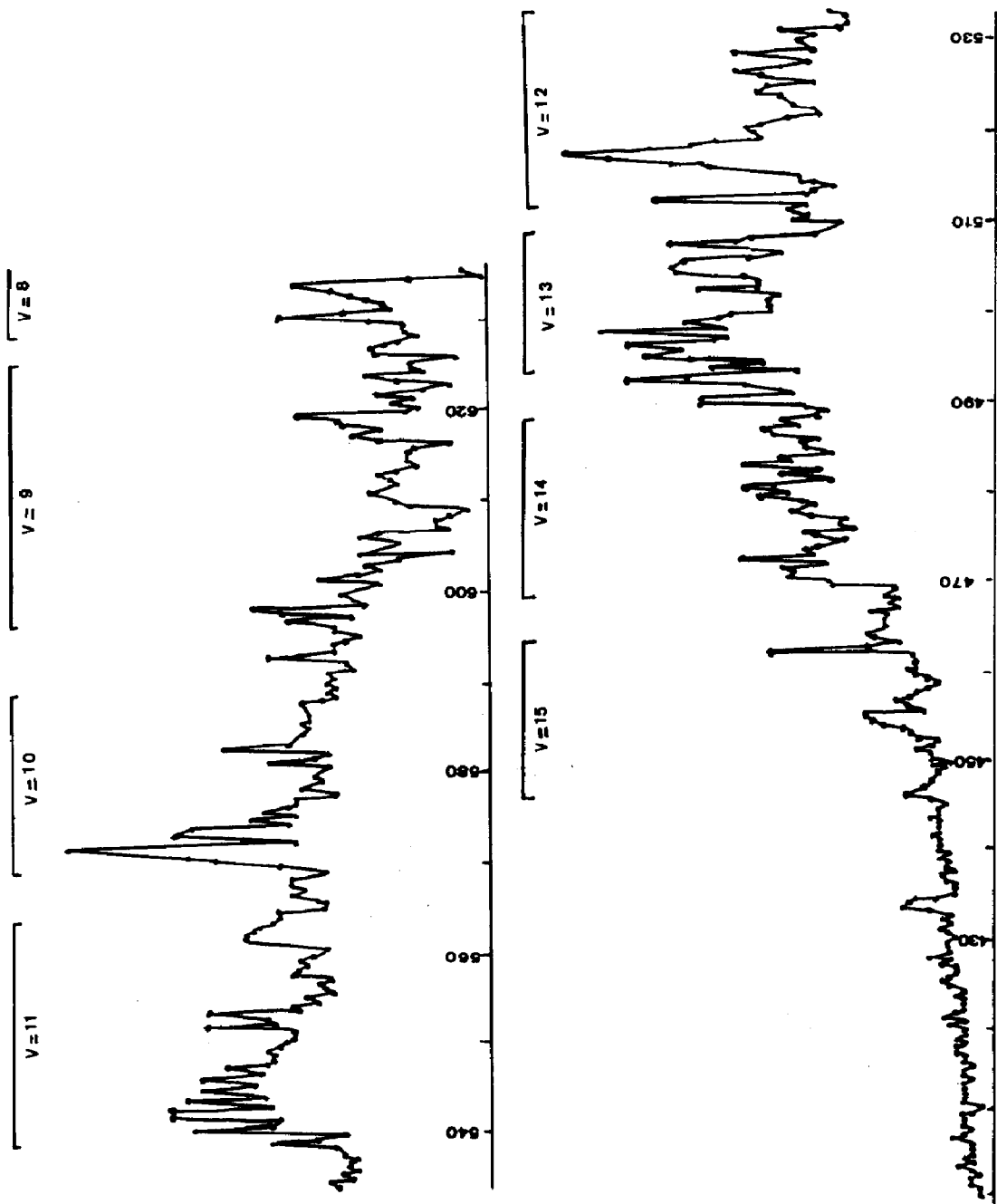Fig. 1. Emission of $NH_2(\tilde{A}\,^2A_1)$ (ammonia pressure, 300 Torr; laser power, 100 W).

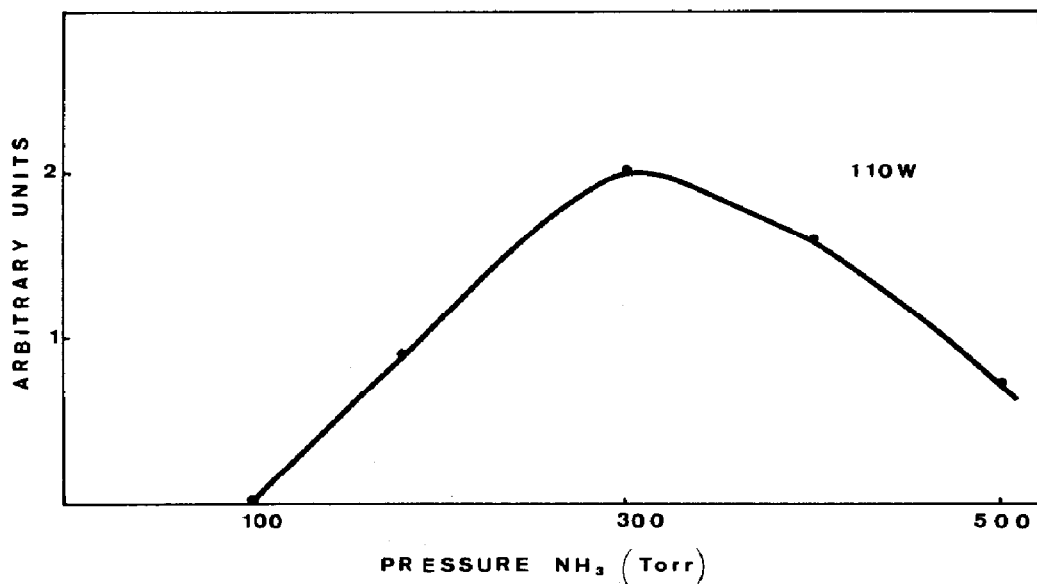Fig. 2. Spectra of $NH_2(\tilde{A}^2A_1 \rightarrow \tilde{X}^2B_1)$ ($P_{NH_3} = 200$ Torr).

4

Fig. 3. Variation in $NH_2(\widetilde{A}\,^2A_1 \rightarrow \widetilde{X}\,^2B_1)$ emission at 530 nm with ammonia pressure.

As the emission from the first ν_2 rovibronic levels corresponds to wavelengths above 650 nm, only transitions corresponding to ν_2 excitation between $v' = 8$ and $v' = 15$ were identified.

The dependence of the signal intensity at $\lambda = 530$ nm on the ammonia pressure exhibits a maximum at about 300 Torr (Fig. 3).
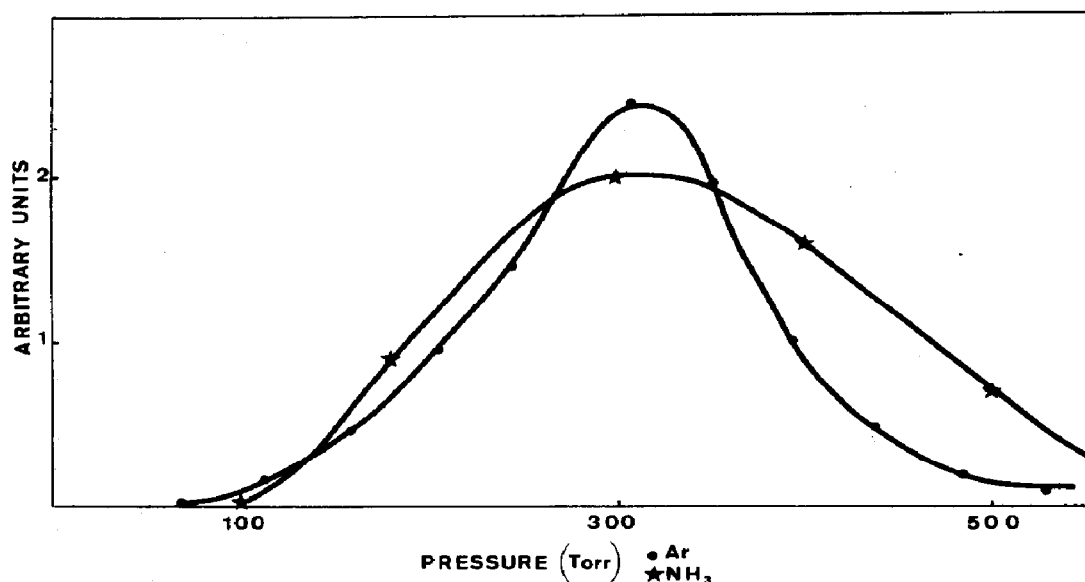

Fig. 4. Variation in $NH_2(\widetilde{A}\,^2A_1 \rightarrow \widetilde{X}\,^2B_1)$ emission with ammonia pressure (★) and argon pressure (●) for $p_{NH_3} = 50$ Torr.

3.2. NH(A $^3\Pi \rightarrow X^3\Sigma^-$) emission

The emission from NH(A $^3\Pi$) at 336 nm was observed concurrently with the NH$_2$($\tilde{A}^2A_1$) emission but the intensity of the NH emission was too weak for accurate rotational analysis of the 0–0 and 1–1 electronic transitions to be carried out.

3.3. Role of transparent and inert gases

The intensity of the luminescence is modified greatly if various gases which are transparent at 10.6 μm are added to the ammonia. For example, no emission occurs when 50 Torr pure NH$_3$ are present. Including 60 Torr argon results in strong luminescence (Fig. 4). Moreover, in the presence of argon, the conic zone of emission extends beyond the focus point (Fig. 5) in the irradiated volume.

Nitrogen does not appear to have any significant effect on the emission at these pressures. In contrast, helium has a dramatic inhibitory effect: there is a marked reduction of the signal when it is added to the ammonia.
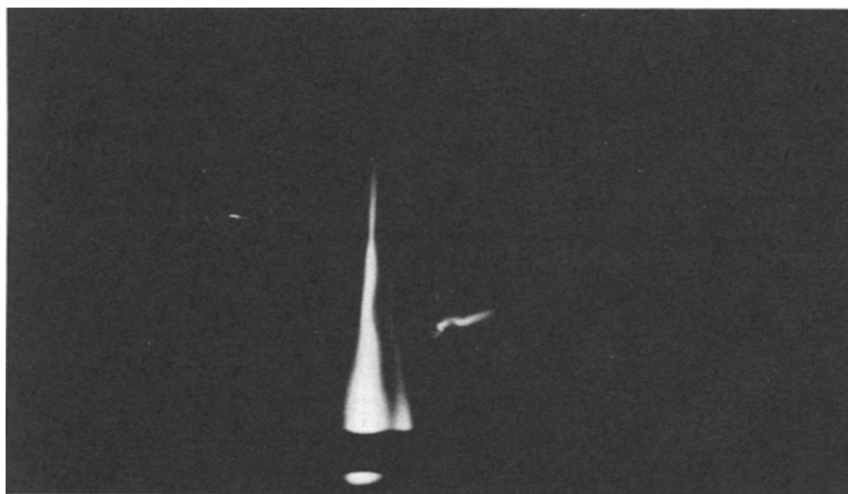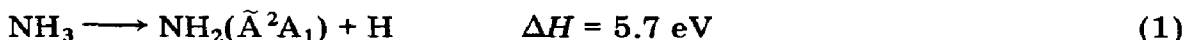

Fig. 5. Emission of NH$_2$($\tilde{A}^2A_1$) (p_{NH_3} = 100 Torr; p_{Ar} = 300 Torr).

4. Discussion

4.1. NH$_2$($\tilde{A}\ ^2A_1 \rightarrow \tilde{X}\ ^2B_1$) formation

The NH$_3$ dissociation process leading to NH$_2$($\tilde{A}^2A_2$) photofragments requires a lot of energy:

$$NH_3 \longrightarrow NH_2(\tilde{A}^2A_1) + H \qquad \Delta H = 5.7 \text{ eV} \qquad (1)$$

The first two potential curves of NH$_3$ describing the NH$_2$ ... H dissociation, suggested by Douglas [19] and theoretically by Runau et al. [20], are illustrated in Fig. 6. They show that the ground state of NH$_3$ ($\tilde{X}^1A_1$), which belongs to the C$_{3v}$ symmetry group, correlates with the dissociation
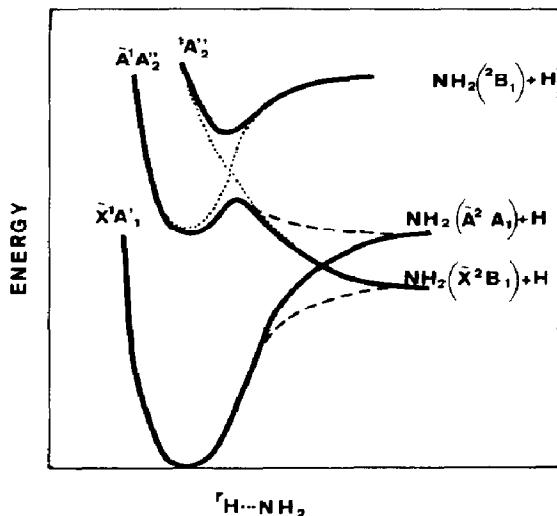
Fig. 6. Potential curves for $NH_3 \rightarrow NH_2 + H$ dissociation for planar NH_3. The dotted curves show the states which form $\tilde{A}^1A_2''$ and the broken curves are for the pyramidal geometry [19].

channel $NH_2(\tilde{A}^2A_1) + H(^2S)$. NH_2 in its ground state ($\tilde{X}\,^2B_1$) is generated from the predissociation of excited states of NH_3 only.

The probability of the formation of $NH_2(\tilde{A}^2A_1)$ was discussed by Douglas [19] on the basis of spectroscopic studies and by Donnelly et al. [10] from their study of excimer laser excitation of NH_3 at 193 nm. It seems that the symmetry of NH_3 is transformed from pyramidal to planar D_{3h} when it enters excited or ionic states. According to Donnelly et al. [10], 98% of excited ammonia in its $\tilde{A}$ state at 5.72 eV possesses $\tilde{A}^1A_2''$ planar symmetry, and thus an intersection between the ground and the $\tilde{A}^1A_2''$ states is allowed. CW IR excitation coupled with the heat bath generated by collisional activation brings a small fraction of the NH_3 molecules (corresponding to the Boltzmann energy distribution tail) to above 4.5 eV. Moreover, for some of the molecules the internal energy may be sufficiently high to allow their dissociation according to reaction (1).

If the $NH_3\,\tilde{A}$ state is pyramidal with $\tilde{A}^1A_1$ symmetry, cross-over between the $\tilde{X}\,^1A_1$ and $\tilde{A}\,^1A_1$ potential curves is forbidden on grounds of symmetry, and consequently only $NH_2(\tilde{X}^2B_1)$ can be formed; unfortunately our experimental set-up does not enable such a ground state radical to be observed.

4.2. NH(A $^3\Pi$) formation

The dissociation process

$$NH_3 \longrightarrow NH(A\,^3\Pi) + 2H(^2S) \qquad \Delta H = 7.45 \text{ eV} \qquad (2)$$

leads to the formation of $NH(A\,^3\Pi)$ but requires a lot of energy. Other parallel dissociative channels leading to less energetic photofragments as $NH(a\,^1\Delta)$ and $NH(b\,^1\Sigma^+)$ can occur. Moreover it is quite possible that other

radical species may act as energy-pooling intermediates. The lifetime of such an intermediate must be long for the collisional excitation to be effective. Therefore the following steps involving the ground state $NH_2(\tilde{X}\,^1B_1)$ and the first excited state $NH_2(\tilde{A}\,^2A_1)$ whose lifetime is about 15 μs [21] may be considered:

$$NH_2(\tilde{X}\,^2B_1) \longrightarrow NH(A\,^3\Pi) + H(^2S) \qquad \Delta H = 7.5 \text{ eV} \qquad (3)$$

$$NH_2(\tilde{A}\,^2A_1) \longrightarrow NH(A\,^3\Pi) + H(^2S) \qquad \Delta H = 6.3 \text{ eV} \qquad (4)$$

It is worth noting that the bending frequencies ν_2 corresponding to $NH_3(\tilde{X}\,^1A_1)$ and $NH_2(\tilde{A}\,^2A_1)$ are very similar while $NH_2(\tilde{X}\,^2B_1)$ species do not absorb at 10.6 μm [22, 23].

From theoretical work concerning the correlation between NH_2 and its dissociation channels $NH + H$, it is possible to predict that $NH(A\,^3\Pi)$ can be formed only from $NH_2(2\,^2A_1)$ at 7.8 eV [24], so the formation of $NH(A\,^3\Pi)$ from $NH_2(\tilde{X}\,^2B_1)$ and $NH_2(\tilde{A}\,^2A_1)$ should be excluded.

Another intermediate species may also be involved in the formation of $NH(A\,^3\Pi)$; recently, an NH_3 triplet located at 5.3 eV, whose symmetry is as yet unknown, was observed [25]. It seems possible, as pointed out previously for SO_2 [26], that an interstate electronic relaxation could bring some molecules into this metastable triplet state. Owing to its long lifetime, this triplet has been detected only by electron impact excitation and has not been observed by optical absorption or emission methods until now. This first ammonia triplet state should act as an energy well, and it is possible for some of the ammonia molecules to reach an energy of 2.08 eV and dissociate as follows:

$$NH_3(T) \longrightarrow NH(A\,^3\Pi) + H_2(X\,^1\Sigma^+) \qquad \Delta H = 2.08 \text{ eV} \qquad (5)$$

4.3. Statistical temperature evaluation

The average temperature inside the irradiated zone can be estimated by considering the laser energy captured in the gaseous medium by absorption and the corresponding heat loss by diffusion.

In the photosteady state assumption, the difference between the absorbed energy Q_L and the heat carried outside the irradiation volume by diffusion is given to a first approximation by the enthalpy variation of the gaseous volume:

$$Q_L - 2\pi\lambda_T[S]\,\frac{\Delta T}{S_c - S_b} = nC_v\Delta T$$

where S_b and S_c (cm^2) are the cross-sections of the beam and the cell respectively and S is the reduced cross-section.

The thermal conductivity λ_T and the heat capacity C_v at constant volume, which are temperature dependent [27], may be calculated by an iterative computational procedure. In this way it is possible to obtain the

average temperature inside the irradiation zone, which under our experimental conditions (p_T = 300 Torr; I_{abs} = 70 W) is estimated to be 3000 ± 300 K.

Having calculated this temperature, it is possible to estimate the fraction of molecules which possess the minimum energy of 5.7 eV required for dissociation reaction (1). For a Boltzmann distribution of energy at 3000 K, under the present experimental conditions (irradiation volume, 7 cm^3; pressure, 300 Torr), about 10^{10} molecules have an energy of more than 5.7 eV and are liable to form $NH_2(\tilde{A}\,^2A_1)$.

4.4. $NH_2(\tilde{A}\,^2A_1 \rightarrow \tilde{X}\,^2B_1)$ emission: dependence on the buffer gas

The $NH_2(\tilde{A}\,^2A_1)$ radical emission intensity *vs.* the total gas pressure passes through a maximum at about 300 Torr. The coupling between the collisional activation and the growing adiabaticity of the gaseous medium increases with the total pressure. Consequently the $NH_2(\tilde{A}\,^2A_1)$ formation is promoted until $NH_2(\tilde{A}\,^2A_1)$ quenching becomes preponderant and depletes the emission intensity.

Addition of argon gas greatly enhances the $NH_2(\tilde{A}\,^2A_1 \rightarrow \tilde{X}\,^2B_1)$ emission (Fig. 4) and consequently the concentration of excited species. It is important to note that the emission remains narrowly confined to the irradiated volume extended beyond the focus point (Fig. 5), indicating the determining role played by collisional interaction between the vibrationally excited NH_3 molecules and the argon buffer gas. As argon is transparent at 10.6 μm, the first photon travels a further distance before it is absorbed than in pure ammonia, leading to the extension of the emission zone.

Since V–T energy transfer is the only possible interaction between excited NH_3 and the rare gases tested, it is obvious that the thermodiffusivity plays a prominent role under these conditions.

The thermodiffusivity χ, which governs the rate of the heat carried out of the irradiated zone by diffusion, is proportional to $\xi\lambda_T/\rho C_p(T)$, with the cell geometry factor $\xi = (\chi/r)^2$. χ is the smallest root of the zeroth-order Bessel function of the first kind (cylindrical cell and laser beam diameter of 1 cm) [28], r (cm) is the cell radius, λ_T (J cm^{-1} K^{-1} s^{-1}) is the thermal conductivity coefficient, ρ (mol cm^{-3}) is the gas density (at 300 Torr = 1.76×10^{-5} mol cm^{-3}) and k (cm^3 mol^{-1} s^{-1}) is the rate constant for the quenching of $NH_2(\tilde{A}\,^2A_1)$ by argon, N_2 or helium.

As shown in Table 1, a satisfying correlation exists between the relative emission intensity observed in the presence of argon or helium and the thermodiffusivity factors of these gases. At a given temperature, the smaller the χ factor the higher is the promoting effect.

Addition of N_2 to NH_3 has no effect on the emission intensity, although the two χ factors are very similar. The nitrogen molecule vibrates at 2360 cm^{-1} and the V–V energy transfer which takes place decreases the collisional activation of ammonia molecules. Nevertheless V–T transfer occurs between excited ammonia and nitrogen. These two effects render the nitrogen gas present in the mixture inoperative.

TABLE 1

Experimental results

	T (K)	C_p/R [a]	$\lambda \times 10^6$ [a] (cal cm^{-1} K^{-1} s^{-1})	$\chi = R\lambda/\rho C_p$ (cal cm^2 K^{-1} s^{-1} mol^{-1})	$k \times 10^{10}$ [b] (cm^3 mol^{-1} s^{-1})
NH$_3$	1000	6.72	369	11.44	
	3000	9.38	1182.3	26.26	5
N$_2$	1000	3.93	158.9	8.42	0.4
	3000	4.45	363.6	17.02	
Ar	1000	2.5	97.9	8.16	1.2
	3000	2.5	199.7	16.64	
He	1000	2.5	825.3	68.77	0.92
	3000	2.5	1676.3	139.70	

$C_p(T)$ (J mol^{-1} K^{-1}), heat capacity; R, gas constant; ρ, gas density (300 Torr) (1.76 $\times$ 10^{-5} mol cm^{-3}); k, rate constant for NH$_2(\tilde{A}^2A_1)$ with argon, N$_2$ and NH$_3$; λ, thermal conductivity.
[a] From ref. 28.
[b] From ref. 21.

Finally, helium strongly quenches the NH$_2(\tilde{A}^2A_1)$ emission by decreasing both the adiabaticity of the system and the signal intensity, which is proportional to the energy density, while nitrogen is ineffective. Otherwise, as indicated in Table 1, the abilities of nitrogen, argon and helium to quench NH$_2(\tilde{A}^2A_1)$ are quite similar, whilst ammonia is five times more efficient as a quencher.

5. Conclusions

The formation of NH$_2(\tilde{A}^2A_1)$ and NH(A$^3\Pi$) from the CW CO$_2$ laser excitation of NH$_3$ has been described. When considering the formation of these excited radicals, it appears that for NH$_2(\tilde{A}^2A_1)$ a cross-over between the first excited state of ammonia and the ground state must be considered. For NH(A$^3\Pi$) a mechanism involving the NH$_3$ triplet state as an energy-pooling system seems possible, but this is more hypothetical.

When transparent gases are added, the NH$_2(\tilde{A}^2A_1 \rightarrow \tilde{X}^2B_1)$ emission is strongly perturbed; this indicates the crucial role played by thermodiffusion in the course of the photoexcitation by a powerful CW IR laser. The addition of argon, or heavier rare gases, strongly promotes certain emissions, and this may be used to study the particular radical mechanism for the selected experimental conditions.

Acknowledgment

References

1 T. G. Slanger and G. Black, *J. Chem. Phys.*, 77 (1982) 2432.
2 J. Masanet, A. Gilles and C. Vermeil, *J. Photochem.*, 3 (1974) 417.
3 A. Gilles, J. Masanet and C. Vermeil, *Chem. Phys. Lett.*, 25 (1974) 346.
4 H. Okabe and M. Lenzi, *J. Chem. Phys.*, 47 (1967) 5241.
5 K. H. Becker and K. H. Welge, *Z. Naturforsch., Teil A*, 18 (1963) 600.
6 K. H. Becker and K. H. Welge, *Z. Naturforsch., Teil A*, 19 (1964) 1006.
7 A. M. Quinton and J. P. Simons, *J. Chem. Soc., Faraday Trans. II*, 78 (1982) 1261.
8 U. Schurath, P. Tiedman and R. N. Schindler, *J. Phys. Chem.*, 73 (1969) 457.
9 M. Suto and L. C. Lee, *J. Chem. Phys.*, 78 (1983) 4215.
10 V. M. Donnelly, A. P. Baronavski and J. R. Donald, *Chem. Phys.*, 43 (1979) 271.
11 V. M. Donnelly, A. P. Baronavski and J. R. Donald, *Chem. Phys.*, 43 (1979) 283.
12 L. Hellner, K. T. Grattan and M. H. Hutchinson, *J. Chem. Phys.*, 81 (1984) 4389.
13 C. Borde, A. Henry and L. Henry, *C.R. Acad. Sci. Paris*, 262 (1969) 1389.
14 J. P. Campbell, G. Hancock, J. B. Halpern and K. H. Welge, *Chem. Phys. Lett.*, 44 (1976) 404.
15 I. Hazanaki, K. Kasatani and K. Kuwata, *Chem. Phys. Lett.*, 75 (1980) 123.
16 P. Avouris, M. T. Loy and I. Y. Chan, *Chem. Phys. Lett.*, 63 (1979) 624.
17 J. Tardieu de Maleissye and F. Lempereur, *Appl. Opt.*, 81 (1982) 334.
18 K. Dresseler and D. A. Ramsay, *Philos. Trans. R. Soc., Ser. A*, 251 (1959) 553.
19 A. E. Douglas, *Discuss. Faraday Soc.*, 35 (1963) 168.
20 R. Runau, S. D. Peyerimoff and R. J. Buenker, *J. Mol. Spectrosc.*, 68 (1977) 253.
21 M. Lenzi, J. R. McNesby, A. Mele and C. Nguyen, *J. Chem. Phys.*, 57 (1972) 319.
22 T. Amano, K. Kawaguchi, M. Kakimoto, S. Aito and E. Hirota, *J. Chem. Phys.*, 77 (1982) 159.
23 J. W. C. Johns, D. A. Ramsay and S. C. Ross, *Can. J. Phys.*, 54 (1976) 1804.
24 R. P. Saxon, B. H. Lengsfield III and B. Liu, *J. Chem. Phys.*, 78 (1983) 312.
25 T. Abuain, I. L. Walker and D. F. Dance, *J. Chem. Soc., Faraday Trans. II*, 80 (1984) 641.
26 C. Lalo, J. Masanet, F. Lempereur and J. Tardieu de Maleissye, *Ber. Bunsenges. Phys. Chem.*, 89 (1985) 299.
27 R. A. Svehla, *NASA Tech. Rep. R. 132*, 1962.
28 R. C. L. Yuan and C. W. Flynn, *J. Chem. Phys.*, 57 (1972) 1316.